High resolution scanning tunneling spectroscopy of ultrathin iron silicide grown on Si(111): Origin of the $c(4\times8)$ long range order

G. Garreau,* S. Hajjar, G. Gewinner, and C. Pirri
Laboratoire de Physique et de Spectroscopie Electronique—CNRS-UMR 7014, Faculté des Sciences et Techniques, 4 Rue des Frères Lumière, 68093 Mulhouse, France
(Received 3 February 2005; published 31 May 2005)

Thin iron silicide grown on Si(111) undergoes a $p(2\times2)\rightarrow c(4\times8)$ ordering process upon annealing that was studied by scanning tunneling spectroscopy. We identify unambiguously 3 nonequivalent Si adatom sites in the $c(4\times8)$ unit cell and a well localized electronic state that exhibits $p1m$ spatial group symmetry as opposed to the 2 sites and $p2mm$ symmetry revealed so far by standard topographs. Amazingly this electronic state originates in an atomic defect in the fifth subsurface layer, right at silicide-substrate interface and the $c(4\times8)$ periodicity reflects long range ordering of these defects.

DOI: 10.1103/PhysRevB.71.193308 PACS number(s): 68.37.Ef, 68.35.Bs, 68.35.Dv, 73.20.−r

Iron silicide growth on Si has attracted a lot of interest in the last decades due to its potential for technological applications as well as the remarkably rich variety of phases that are exciting to investigate from a fundamental point of view.[1] Indeed, besides the bulk stable β-$FeSi_2$ and α-$FeSi_2$ phases, metastable Fe silicides have been synthesized by epitaxy on Si(111). In particular, typical phases grow with cubic CsCl-type $FeSi_x$ structure in which randomly distributed Fe vacancies are progressively formed when the stoichiometry evolves from FeSi to $FeSi_2$.[2] Sirringhaus *et al.*[3] suggested that these Fe vacancies could be responsible for the atomic-scale contrast variations observed in scanning tunneling microscopy (STM) images for thin iron silicide films. Indeed, although these silicide layers are terminated by a $p(2\times2)$ Si adatom network, 2 nonequivalent adatom sites—bright and dark atoms—were observed on the STM images. These sites are either randomly distributed[3–7] or well ordered[6,7] depending both on the nominal Fe thickness and annealing temperature. In particular, for about 1.6 ML Fe coverage, a homogeneous silicide exhibiting a $p(2\times2)\rightarrow c(4\times8)$ periodicity change upon annealing at higher temperature (800 K) has been observed by STM and low energy electron diffraction (LEED).[6,7] From outstanding STM topographs analysis Krause *et al.*[7] obtained several structural features of the $p(2\times2)$ and $c(4\times8)$ phases, as discussed below. Nevertheless, although defects have been invoked as a possible cause of the atomic-scale contrast variations in the STM topographs, this could never be demonstrated convincingly up to now.

In this paper, we investigate the electronic structure of $p(2\times2)$ and $c(4\times8)$ ultrathin iron silicide layers by means of atomically resolved scanning tunneling spectroscopy (STS) experiments. We demonstrate that STS provides decisive information on the origin of the $c(4\times8)$ order. A simple structural model of the $c(4\times8)$ silicide can be inferred from our striking high resolution STS data. We show in particular that the $p(2\times2)\rightarrow c(4\times8)$ periodicity change results from an ordering of atomic defects located right at the buried silicide/Si substrate interface i.e., as deep as 5 atomic layers below the surface.

Sample preparation, STM and STS experiments were carried out under ultrahigh vacuum. Iron silicide films were grown on Si(111) wafers by solid phase epitaxy as described previously.[6] Topographic and spectroscopic images were acquired at RT in the constant-current mode and current imaging tunneling spectroscopy mode (CITS), respectively.[8] In this last mode, an I–V curve is recorded at every pixel within a constant-current topograph (CCT). Consequently, current images (CIs) for sample voltage (V_S) between −2 and +2 V and CCT of the same area are collected simultaneously at a fixed tip-sample distance determined by the feedback stabilization voltage V_{Sta} and current I_{Sta}.

First, let us summarize the previously published results concerning the $p(2\times2)$ and $c(4\times8)$ homogeneous silicide layers. From step height measurements of CCTs, Krause *et al.*[7] first concluded that the silicide contains 2 unfilled Fe atomic layers and 3 Si atomic layers (result 1). To reach this conclusion they assumed in particular the following features: (i) the silicide is terminated by 2 Si atomic planes, namely a $p(2\times2)$ Si adatom arrangement on top of a $p(1\times1)$ Si plane and (ii) the silicide atomic structure is of cubic CsCl $FeSi_x$ type. We previously confirmed by means of ion scattering spectroscopy the pertinence of the first assumption.[6] Moreover recent x-ray photoelectron diffraction (XPD) experiments show that, although strong vertical relaxations are present in this ultrathin silicide layer, its total thickness and atomic structure is fairly consistent with the model of Krause *et al.*[9] Thus, the first conclusion (result 1) arrived at by Krause appears to be fairly well established. Then, Krause *et al.*[7] showed from CCTs analysis that the Si adatoms reside in T4 coordination sites (result 2). Yet since total energy calculations performed on a CsCl FeSi layer terminated by a $p(2\times2)$ Si adlayer indicate that the H3 site should be energetically favored with respect to the T4 site, Krause *et al.*[7] suggested that each adatom is located on top of a Fe vacancy (result 3). Again, results 2 and 3 are indeed supported by our XPD analysis.[9] Yet, in spite of the unraveling of these three major features (results 1, 2, and 3) of the silicide atomic structure, it was not possible up to now to elucidate the origin of the remarkable $c(4\times8)$ long-range order.

Major insight into this question is obtained by considering Fig. 1 that contains four images collected in the CITS mode for a 1.7 ML Fe-thick silicide. As discussed previously,[6,7]

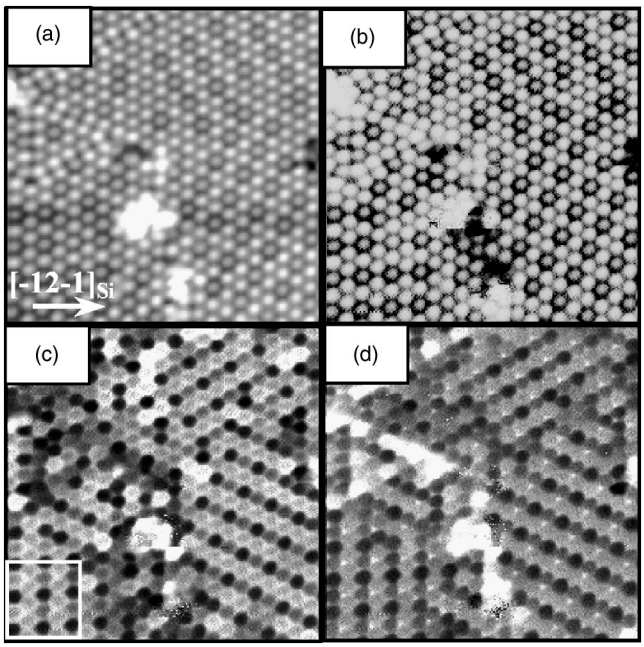

FIG. 1. Constant-current topograph, CCT (a) and current images, CIs (b–d) collected on the same area (14 nm×14 nm) of an ultrathin iron silicide (t_{Fe}=1.7 ML, annealing at 800 K for 20 min). (a) Empty-state CCT (V_{Sta}=+1.89 V, I_{Sta}=0.1 nA), CI: (b) V_S=−0.75 V, (c) V_S=+0.93 V, and (d) V_S=+1.49 V. The different CI were measured with a stabilization voltage and current of 1.89 V and 0.1 nA, respectively. Each image contains 300×300 pixels.

empty state CCT [Fig. 1(a)] reveals a $p(2\times2)$ Si adatoms network and two types of adatoms are clearly visible. More specifically, one-fourth of the adatoms appear to be depressed (dark) in comparison to the others. The major part of the surface thus presents rotationally equivalent domains in which the atomic-scale contrast variations reflect a $c(4\times8)$ superstructure. Figure 1(a) shows mainly three $c(4\times8)$ domains, rotated with respect to each other by 120°. Let us note here that these domains display *p*2*mm* symmetry in CCT mode whereas an atomic structure for the whole silicide film based on the model of Krause *et al.* is expected to belong to the *p*1*m* spatial group. On sparse areas of the surface the dark and bright adatoms are randomly distributed. This merely reflects an incomplete ordering process due to the relatively low annealing temperature. Whereas the CI at negative sample bias [Fig. 1(b)] gives the same information as the CCT, Fig. 1(c) clearly reveals that there are actually not 2, as believed up to now, but 3 different adatom types (labeled A, B, and C). To show this more strikingly and gain quantitative information on their respective electronic structure, the normalized tunneling differential conductivity $(dI/dV)/(I/V)$ has been calculated numerically for each adatom type in Fig. 2. Although this quantity is not merely proportional to the surface local density of states (LDOS), the sharp features in the normalized tunneling spectrum and in the LDOS are generally located at the same energies.[8] Since our normalized differential conductance $(dI/dV)/(I/V)$ spectra present sharp peaks, we assume that they reflect essentially the LDOS, as usually done in the literature.[10]

From −1.7 eV to +0.5 eV the three spectra are fairly similar, exhibiting two common peaks at ∼−0.8 eV and

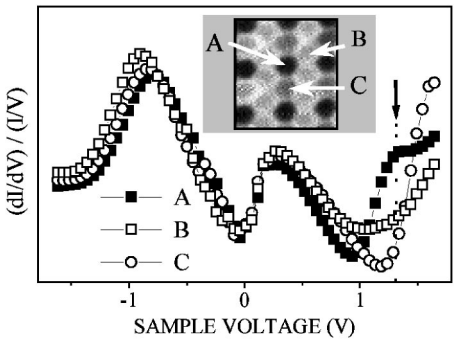

FIG. 2. Normalized differential tunneling conductance versus sample bias collected on the distinct adatom sites A, B, and C visualized on the CI (inset) that corresponds to the small square (bottom left corner) of Fig. 1(c). Each curve has been obtained by the numerical differentiation of the current integrated over small square area (1×1 Å^2) centered on the different adatom sites.

∼+0.3 eV. This similarity explains why the $c(4\times8)$ modulation is barely visible in the filled-state CCTs.[6,7] Yet major spectroscopic differences between the three sites can be seen above +0.5 eV. In particular, the LDOS between 1.1 and 1.4 eV is definitely larger for site A than for the two other sites.

Besides the existence of 3 rather than 2 different adatom sites, another important result concerns the symmetry group of the $c(4\times8)$ phase. Indeed, as compared to CCTs, Figs. 1(c), 1(d), and 3(a) reveal that one mirror symmetry is definitely broken in the current maps i.e., the spatial group is lowered to *p*1*m*. For instance, if we concentrate on the primitive unit cell shown as a dashed rectangle in Fig. 3(a) it appears that only the (10-1) mirror plane is left. Its intersection with the image plane is parallel to the dotted straight line.

Further decisive insight into the surface electronic structure is obtained by investigating systematically the LDOS as a function of position in high resolution CIs (Fig. 3). We find that for each pixel in a well-defined area and only in this area of the unit cell the LDOS presents a peak at ∼+1.3 eV, i.e., at the same energy as at site A. Moreover the intensity of this state strongly depends on the location inside this area that extends over the dotted "ice cream cone" depicted in Fig. 3. Note that this cone has a definite orientation that points into [-12-1] direction of the Si (111) substrate. The peak intensity is maximal between positions 1 and 2. Its value is the same for symmetric positions with respect to a (10-1) mirror plane but decreases drastically as soon as one moves out of this plane. Note that the lowered *p*1*m* symmetry is very nicely confirmed by this remarkable "ice cream cone" shape since the measured LDOS associated with the 1.3 eV surface state directly reflects its charge distribution in real-space.

Additionally, we observe first that, even if the sites A are randomly distributed, either isolated or forming locally lines or clusters of two or three adjacent A adatoms, the highly localized surface state still exists and can be systematically related to a site of type A. This can be seen by comparing Figs. 1(b) and 1(d) if one notes that a cone of the surface state real-space charge distribution coincides with a small white spot in Fig. 1(d). Second, as discussed in Ref. 6, the density of sites A is the same for both $p(2\times2)$ and

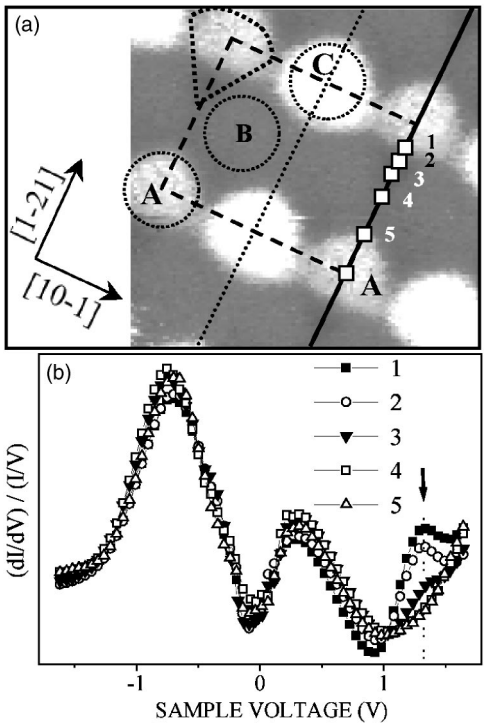

FIG. 3. (a) High resolution tunneling current map of a small (26 Å$\times$26 Å) $c(4\times8)$ iron silicide area ($t_{Fe}\sim1.7$ ML, annealing at 800 K for 20 min). The image contains 110×110 pixels. The in-plane orientations were determined from the initial 7×7 Si(111) substrate. The three dotted circles are centered on the different adatom sites A, B, and C. The dashed rectangle indicates the unit cell of the $c(4\times8)$ periodicity. The dotted straight line is the intersection between the surface plane and the (10-1) mirror plane. For each pixel inside the dotted "ice-cream cone" shape area the normalized differential conductance spectrum presents a feature around +1.3 V. (b) Normalized differential tunneling conductance for each position (1–5) marked on (a). The arrow indicates the position of the empty localized state. Each spectrum was obtained from the tunneling current integrated over the small white squares (1×1 Å^2) of (a).

$c(4\times8)$ phases, which strongly suggests that the periodicity change versus annealing temperature is just an ordering of the same number of A sites with their closely tied highly localized surface state. Since the LDOS is independent on long-range order, it must be the signature of a characteristic local atomic arrangement underneath and in close proximity to an adatom of type A. This strongly suggests that this specific A site local atomic arrangement reflects the presence of an atomic defect in close proximity.

Indeed, if one assumes a defected CsCl based structure, any model has to take into account the number of missing Fe atoms in the silicide. Unfortunately this number cannot be determined precisely since it depends too critically on the minimal nominal Fe thickness for which the silicide covers entirely the Si substrate. This thickness can be reasonably estimated to be 1.6(±0.1)ML.[6,7] Hence, the number of missing Fe atoms inside the $c(4\times8)$ unit cell is about 6 ± 2. As mentioned above, 4 Fe vacancies are located in the top Fe layer, below each Si adatom. Thus, 2 ± 2 missing atoms remain to be placed in the two Fe layers. These additional

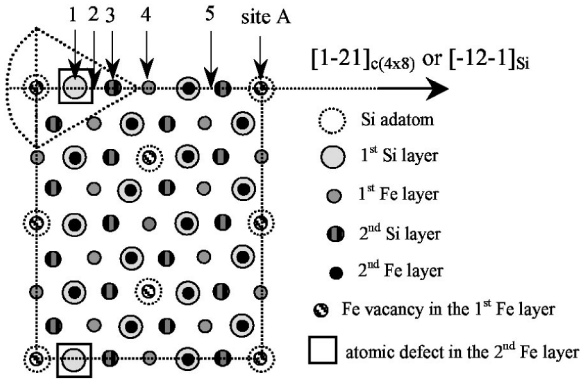

FIG. 4. One atomic defect model of the $c(4\times8)$ phase: the 5 surface layers are projected onto the (111) plane. The dashed rectangle corresponds to the unit cell of the $c(4\times8)$ periodicity. The different positions (1–5) and the dotted "ice-cream cone" shape area are the same as the ones of Fig. 3(a). The in-plane orientation of the silicide with respect to the Si substrate (interface of type B) was determined previously by XPD (Ref. 9).

missing atoms can correspond either to Fe vacancies or possibly substitutional Si atoms. In both cases, we are left with an atomic defect in the relevant Fe atomic layer. For stability reasons one also expects the additional defects to be located in the bottom Fe layer rather than the top Fe layer where there are already 4 of them.

It appears that we are led to a very simple structure if there is just one additional atomic defect per unit cell. Indeed the only possible location of the atomic defect that is consistent with the $p1m$ spatial symmetry group and observed orientation of the "ice cream cone" is in the bottom Fe atomic layer as depicted in Fig. 4. Note that no similar low symmetry position can be found in the top Fe layer. It is very remarkable that a defect located four atomic layers below the topmost atomic layer clearly reflects in the LDOS probed by STM or STS. The effect is most likely indirect by defect-induced local atomic relaxation that propagates to the surface and changes markedly the surface electronic structure and atomic positions near the type A adatom. Simple LEED observations strongly support the fact that the $c(4\times8)$ actually originates in the deepest layers of the silicide.[9] Indeed, we observe that after the deposition at RT of 2 ML Fe on the homogeneous $c(4\times8)$ silicide, a fairly sharp $p(1\times1)$ pattern is visible at low beam energies whereas a $c(4\times8)$ pattern is still visible at energies higher than 150 eV. Yet, at low beam energies, typically 40 eV, the high elastic reflectivity and short inelastic electron mean free path imply that LEED probes long range order in two or three topmost layers only, whereas at higher energies deeper layers are probed too. This suggests that the Fe-rich silicide formed after additional deposition of 2 ML Fe consists basically of two silicide layers, one of $p(1\times1)$ periodicity on top of a $c(4\times8)$ periodic one. Since because of the high reactivity of Fe and Si at RT, at least the three topmost atomic layers of the initial $c(4\times8)$ silicide undergo a reorganization of the Si and Fe species as well as defects, the initial $c(4\times8)$ periodicity can hardly originate in these atomic layers only.

If the unit cell contains more than one ordered additional atomic defect, more complex structural models might be in-

voked. However, as mentioned above, the defect-induced perturbation in surface electronic structure is a very local property. Hence one would expect the defects to form a cluster around the projection of an A site in fifth plane. A possible example is a complex of 3 defects centered on an A site. This means adjacent defects in nearest in-plane neighbor positions of the Fe bottom plane and is likely to be energetically unfavorable. Actually, the CIs in Fig. 1 clearly show triangular clusters of 3 adjacent A sites that would imply a very large unrealistic number of adjacent defects. In this respect, note instead the relevant "ice cream cone" orientations that can be readily understood in above one defect model if there exists a strong repulsive interaction between defects. For a 3 defects complex per A site there is also local threefold symmetry which is at odds with the observed "ice cream cone" shape. Similarly a 2 defects complex per A site seems also hardly compatible with this shape. Therefore, a model that contains more atomic defects appears to be quite unlikely.

In summary, the surface electronic structure of the ultrathin iron silicide layer that exhibits a $p(2\times2)\rightarrow c(4\times8)$ periodicity change versus annealing temperature has been investigated by STS. Our high resolution data reveal that the $c(4\times8)$ surface structure belongs actually to the $p1m$ spatial group as expected for a structure based on cubic CsCl-type. We definitely show that, amazingly, an empty spatially localized electronic state probed by STM and STS originates from an atomic defect located as deep as the fifth subsurface atomic layer. The thermally induced periodicity change merely results from a long range ordering of these atomic defects right at the silicide/Si substrate interface and a simple atomic model for the $c(4\times8)$ surface silicide can be proposed. Unfortunately, further quantitative test of this large surface mesh structure by standard surface crystallographic techniques or by realistic surface electronic structure calculations seems by now out of reach.

The authors thank the Centre National de la Recherche Scientifique and Région Alsace for financial support.

*Electronic address: g.garreau@uha.fr

[1] See for instance, I. Goldfarb, Surf. Sci. **554**, L87 (2004), and references therein.
[2] K. L. Whiteaker, I. K. Robinson, C. Benson, D. M. Smilgies, N. Onda, and H. von Känel, Phys. Rev. B **51**, 9715 (1995).
[3] H. Sirringhaus, N. Onda, E. Müller-Gubler, P. Müller, R. Stalder, and H. von Känel, Phys. Rev. B **47**, 10 567 (1993).
[4] A. L. Vasquez de Parga, J. de la Figuera, C. Ocal, and R. Miranda, Europhys. Lett. **18**, 595 (1992).
[5] A. Wawro, S. Suto, R. Czajka, and A. Kasuya, Phys. Rev. B **67**, 195401 (2003).
[6] S. Hajjar, G. Garreau, S. Pelletier, D. Bolmont, and C. Pirri, Phys. Rev. B **68**, 033302 (2003).
[7] M. Krause, F. Blobner, L. Hammer, K. Heinz, and U. Starke, Phys. Rev. B **68**, 125306 (2003).
[8] *Scanning Tunneling Microscopy and Spectroscopy*, edited by D. A. Bonnel (VCH, New York, 1993).
[9] S. Hajjar, Ph.D. thesis, Mulhouse University, 2004 (unpublished).
[10] O. Gurlu, H. J. W. Zandvliet, and B. Poelsema, Phys. Rev. Lett. **93**, 066101 (2004).